American Heart Journal
Founded in 1925

January 1997 Volume 133, Number 1

CLINICAL INVESTIGATIONS

Imaging/Diagnostic Testing

Are soft echoes really soft? Intravascular ultrasound assessment of mechanical properties in human atherosclerotic tissue

Takafumi Hiro, MD, Cyril Y. Leung, MD, Sarah De Guzman, MD, Vincent J. Caiozzo, PhD, Ali R. Farvid, BA, Houshang Karimi, BA, Richard H. Helfant, MD, and Jonathan M. Tobis, MD
Irvine, Calif.

To examine the accuracy of intravascular ultrasound (IVUS) in assessing the biophysical properties of atherosclerotic plaque, 33 human iliac arteries were imaged with a 25 MHz IVUS transducer and classified into four groups on the basis of IVUS appearance: minimally diseased arterial wall, bright echogenic plaque with acoustic shadowing, bright echogenic plaque without shadowing, and hypoechogenic plaque (so-called "soft echoes"). The hardness of each plaque was assessed with an ultrasensitive compression ergonometer. The radial static stress-strain relations fit well ($r > 0.98$) to exponential curves, providing a compression stiffness constant (K) defined as the coefficient of the exponential power. K for bright echogenic plaque with shadowing was significantly greater than that of the other tissues. However, K among minimally diseased entire arterial wall, hypoechogenic plaque, and bright echogenic plaque without shadowing was not significantly different, but these tissues are not physically soft compared with adipose tissue. Therefore, tissue characterization by IVUS distinguishes calcified from noncalcified plaque and accurately predicts its biomechanical hardness. However, soft echoes, although less firm than calcium, do not necessarily correspond to soft tissue. (Am Heart J 1997;133:1-7.)

Intravascular ultrasound (IVUS) imaging provides a detailed structure of arterial cross-sectional anatomy with accurate representation of atherosclerotic plaque dimensions in vitro.[1-10] In addition to the ability to measure plaque size, IVUS image patterns may correspond with the composition of atherosclerotic plaque defined by histologic findings.[2, 3, 8, 11-14] IVUS is also used as a guide for interventional strategies such as balloon angioplasty, directed or rotational atherectomy, and stent deployment.[15-19] Because these interventions respond differently to various tissue components,[15] understanding the mechanical properties of the plaque may be useful in choosing an interventional strategy. Biomechanical properties of atherosclerotic plaque are determined by the composition of the tissue and its spatial distribution in the plaque.[20, 21] By the process of tissue characterization, IVUS may distinguish calcification, fibrosis, or fatty plaque; IVUS may therefore be able to predict the mechanical properties of atherosclerotic plaque.[22]

Previous studies comparing the echogenic patterns of IVUS images with histologic plaque composition distinguished three types of echo patterns and their tissue counterparts: hypoechogenic areas that correspond to lipid-laden zones, echo intensity that is equal to or greater than the reflections from surrounding adventitia and corresponds to fibrous tissue, and intense echogenic structures with acoustic shadowing that correspond to calcification on histologic examination.[2, 3, 8, 11-14] When describing the echogenicity of IVUS images, some authors use a convenient shorthand by referring to the IVUS

From the University of California–Irvine and Orange County's Coroners Office.

Supported in part by National Institutes of Health Grant R01-HL45077-03.

Received for publication March 4, 1996; accepted April 15, 1996.

Reprint requests: Jonathan M. Tobis, MD, Department of Medicine/Cardiology, University of California–Irvine, Bldg. 53, Rte. 81, Room 100, 101 The City Drive South, Orange, CA 92668-3298.

0002-8703/97/$5.00 + 0 4/1/75874

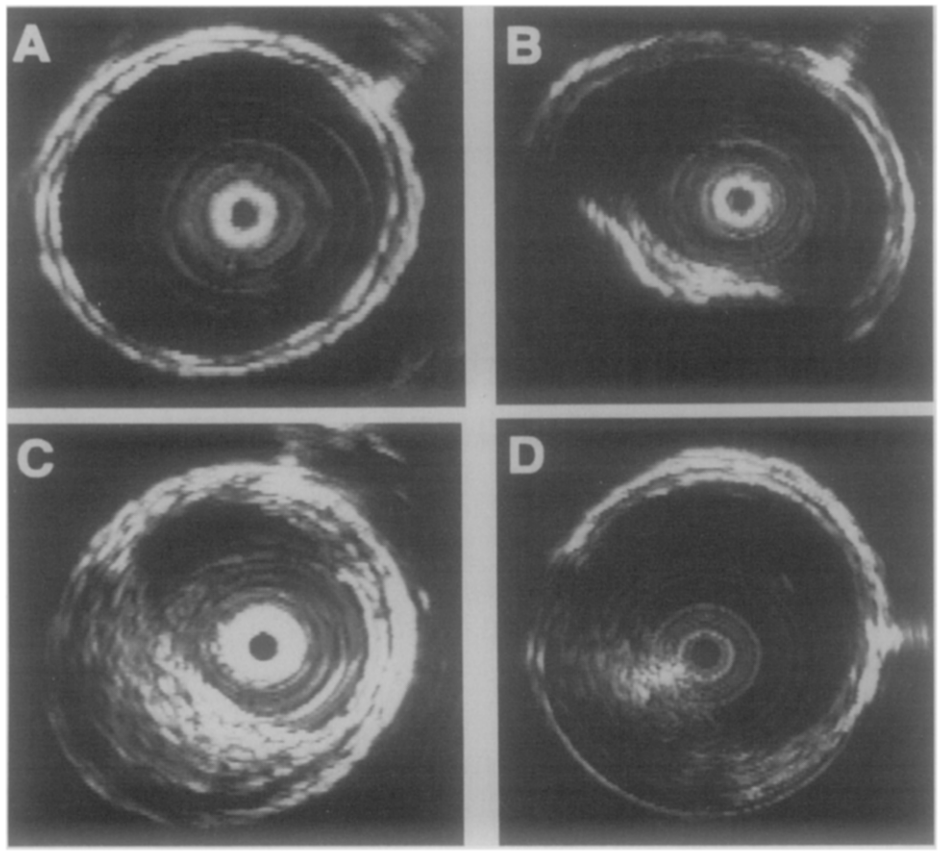

Fig. 1. IVUS classification of plaque. **A,** Normal or minimally diseased arterial wall. **B,** Bright echogenic plaque with shadowing. **C,** Bright echogenic plaque without shadowing. **D,** Hypoechogenic plaque.

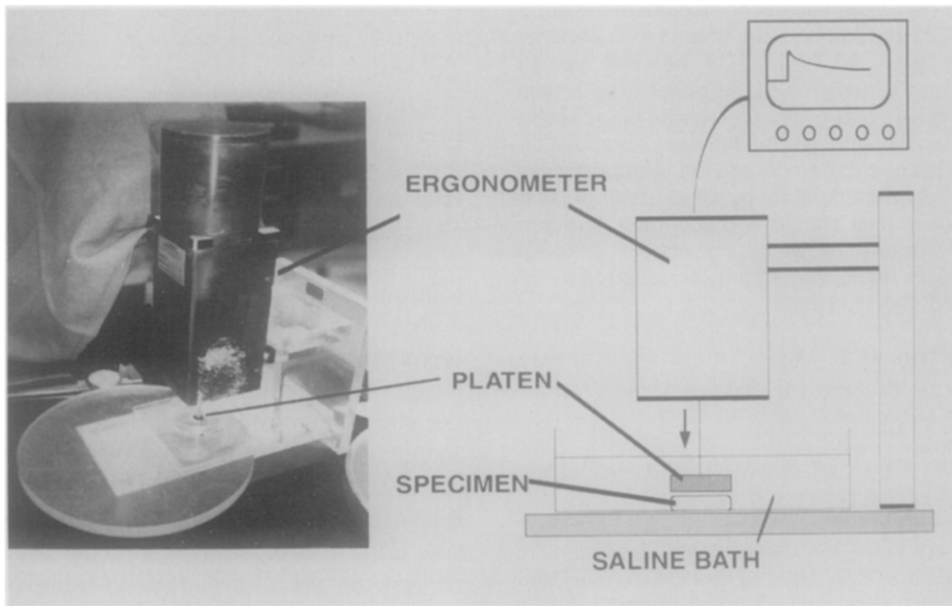

Fig. 2. Servo-controlled mechanical compression ergonometer.

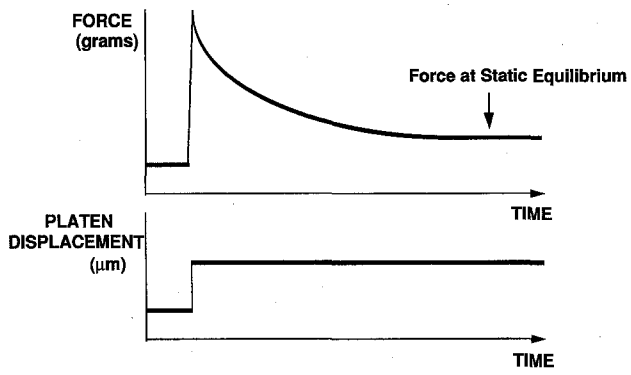

Fig. 3. Time curve of generated compression force after increment of strain *(top graph)*. Platen displacement measured in micrometers, which induces alteration in stress *(bottom graph)*.

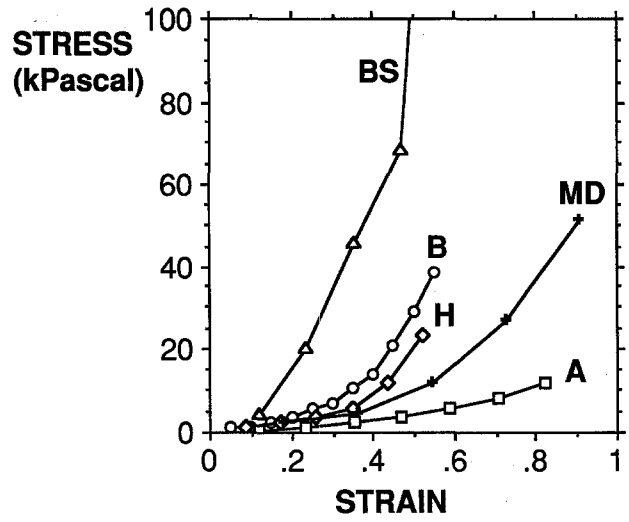

Fig. 4. Example of stress-strain relation for plaque from each group defined by IVUS. 1 kPa = 9.81 g/mm^2; strain = Δ thickness/original thickness. *BS*, Isolated bright echogenic plaque with shadowing; *B*, isolated bright echogenic plaque without shadowing; *H*, isolated hypoechogenic plaque; *MD*, normal or minimally diseased entire arterial wall; *A*, adipose tissue.

images as containing soft echoes. However, differences in how the nomenclature is used exist. Some authors refer to soft echoes as any tissue that is not calcified.[23-25] Other authors refer to soft echoes only when the echo pattern is hypoechogenic compared with the fibrous adventitia.[26-33] The implication is that soft echoes predict soft tissue, that is, lipid-laden plaque. However, the hardness of atherosclerotic plaques has not been assessed in comparison with IVUS images of intact coronary and peripheral vessels. The purpose of this study was to examine whether the descriptors of tissue components by IVUS could predict the mechanical properties of human peripheral atherosclerotic plaque in vitro.

METHODS

Human artery specimens. Thirty-three human iliac arteries approximately 5 cm in length were excised from 18 patients (aged 21 to 85 years) at necropsy in the Orange County Coroner's Office. Because the specimens were obtained from the coroner's office, no clinical information was available. The specimens were immediately preserved in normal saline in a refrigerator. Arteries with visible distortion, surface fracture, overlying thrombus, or large side branches were excluded. To quantitate the relative stiffness of physically soft tissue, six samples of pure adipose tissue from subcutaneous areas were also obtained. To enhance the measurement accuracy, iliac artery plaques were selected to provide large and flat specimens that approximated the size of the platen on the mechanical compression device.

IVUS imaging studies. At the time of ultrasound imaging, the arteries were not preserved in formalin. An 8F guiding catheter was inserted into the proximal end of the vessel, and normal saline was perfused at 100 mm Hg at room temperature. A 3.9F, 25 MHz IVUS catheter (Model 3003, InterTherapy/CVIS, Sunnyvale, Calif.) was used. The entire length of the artery was initially imaged to find an optimal portion of atherosclerotic plaque that provided no significant change in tissue composition or structure within at least a 1 cm length of the artery. Surgical needles were then sutured into the arterial wall opposite the plaque of interest and at the center of the arterial segment of 1 cm length. The needles served as acoustic and physical references to compare the same cross-section among IVUS imaging, mechanical testing, and histologic examination. The images were optimized under visual inspection by manipulating the system settings. The gain settings were determined with the intent of maximizing image morphologic characteristics without excessive dropout, not saturating adventitial intensity, and minimizing noise. On the instrument used in this study, the ramp setting is constant and cannot be varied. Care was taken to position the catheter centrally and coaxially.

The images were stored on S-VHS videotape and interpreted by two investigators without any knowledge of the histologic or mechanical test results. The images of arterial wall were classified into four categories of tissue type on the basis of their appearance by IVUS (Fig. 1). (1) Normal or minimally diseased arterial wall (n = 9): defined as an intact arterial wall with a three-layer appearance with inner and outer bright signals separated by a hypoechogenic layer. (2) Bright echogenic plaque with acoustic shadowing (n = 10): defined as an area of high echo intensity, greater than the adventitia, with acoustic shadowing peripherally. (3) Bright echogenic plaque without acoustic shadowing (n = 8): defined as an area of high echo intensity, equal to or greater than that of the adventitia, without acoustic shadowing. (4) Hypoechogenic plaque (n = 6): defined as an

Table I. Stiffness constant (K) for each group classified by IVUS

		IVUS class			
	Adipose tissue	*Minimally diseased entire arterial wall*	*Bright echogenic plaque without shadowing*	*Hypoechogenic plaque*	*Bright echogenic plaque with shadowing*
K	2.8 ± 1.1*	5.2 ± 0.7	6.2 ± 1.9	6.7 ± 1.6	13.1 ± 5.1†

Values are mean ± SD.
*Adipose tissue vs bright echogenic plaque without shadowing or hypoechogenic plaque, $p < 0.05$.
†Bright echogenic plaque with shadowing vs adipose tissue, minimally diseased entire arterial wall, or bright echogenic plaque without shadowing, $p < 0.0001$. Bright echogenic plaque with shadowing vs hypoechogenic plaque, $p < 0.0005$.

area of low echo intensity (black or speckled grey and black regions).

The arterial images with the needle acoustic reference were digitized with a frame-grabbing board (RasterOps 24STV with software by MediaGrabber, Santa Clara, Calif.) into a Macintosh IIci computer. An on-screen image analysis application (NIH image) was used to measure an objective intensity index for each plaque. The intensity index (II) was calculated as: II = (Iplq – Ibkg)/(Iad – Ibkg), where Iplq was the average videointensity of the plaque, Ibkg was the average background videointensity, and Iad was the average videointensity of the adventitia. The background intensity was obtained from an ultrasound image without an artery in place at the approximate position where plaque would be and with the same system settings. The videointensity had a gray scale of 256 levels on a 640 x 480 pixel display.

Mechanical testing. Mechanical testing was performed within 24 hours after IVUS imaging. The arteries were incised longitudinally along the wall opposite to the plaque, and the cut ends were laid open. A sharp-margined circular stamp bit with a 7 mm diameter (Hollow Punch Set Model 6PC, ToolShack, Long Beach, Calif.) was used to punch out the plaque area of interest. If the punched-out plaque was visually nonuniform, the artery was excluded from study. Except for the normal or minimally diseased arterial wall segments, the plaque was dissected free from the media and adventitia. Both the normal or minimally diseased arteries determined by IVUS and adipose tissue were used in this study as reference to compare their mechanical properties with the atherosclerotic plaques.

An ultrasensitive, servo-controlled mechanical compression ergonometer with a uniaxial displacement resolution of 10 μm (Model 360 ergonometer with Model 310 servo controller, Cambridge Technology Inc, Watertown, Mass.) was used to obtain the stress-strain relation for each tissue. The plaque segment was bathed in room-temperature normal saline and held between the flat hard bottom of the bath and a 7 mm in diameter cylindrical hard plastic platen that was connected to the ergonometer (Fig. 2). Compression of the plaque was uniaxial and perpendicular to the plaque surface. As the platen was advanced on the specimen, the starting point initial thickness was defined as the thickness that yielded a distinct compression force. The compression force was measured with a resolution of 1 gm after the platen compressed the specimen with an incremental length of 50 to 100 μm up to 50% to 95% of initial thickness. The compression force initially generated a peak value, after which the force decreased and reached a static equilibrium (creep) (Fig. 3). The equilibrium was defined as the point in time when the change in force was <2% of the final equilibrium force.

The static equilibrium force in grams was divided by the surface area of the plaque to obtain the radial stress (kpascal) of the plaque. The strain (ΔL/L) was calculated as the value of incremental change in thickness divided by the initial thickness. The measurements were stopped when the plaque showed evidence of mechanical destruction such as cracks, oozing of the lipid component around the tissue, or when the generated force went off scale.

Histologic study. After IVUS imaging and mechanical testing, the punched-out artery specimens were fixed in 10% formaldehyde for at least 24 hours, embedded in paraffin, and processed for histologic examination. The specimens were stained with Masson's trichrome stain and hematoxylin-eosin. To compare the histologic classification with the ultrasound descriptors, a simplified three-category histologic classification was generated. (1) Calcified plaque: plaque with continuous calcification >50 μm.[12] (2) Fibrous plaque: histologic areas of either fibroacellular, hypocellular, or fibrocellular matrix. (3) Fatty plaque: areas with a mixture of fibro-fatty tissue.

Statistics. Values were expressed as mean ± SD. Analysis of variance with the Bonferroni post hoc test was used to compare the mean values among groups. The nonlinear relation between stress and strain was analyzed by the least square method fit to an exponential curve. In these analyses, $p < 0.05$ was considered significant.

RESULTS

Nonlinear stress-strain relation. Thirty-three specimens were available for complete analysis. The mean initial thickness of the specimens was 1.7 ± 0.4 mm (range 0.9 mm to 3.1 mm). The peak static stress obtained was 67 ± 68 kPa (range 2 to 340 kPa). Fig. 4 shows an example of the stress-strain relation for each group of specimens. The stress-strain curve for all the specimens had no linear portion but were well fitted ($r > 0.97, p < 0.05$) to exponential curves: Stress (kPa) = $Ce^{K(strain)} - 1$, where K represents the uniaxial compression stiffness constant, and C = 1 kPa.

Table II. Sensitivity of IVUS for identifying histologic type of plaque

	Ultrasound descriptors		
Histologic class	*Bright echogenic plaque with shadowing*	*Bright echogenic plaque without shadowing*	*Hypoechogenic plaque*
Calcified plaque	91%	9%	0%
Fibrous plaque	0%	50%	50%
Fatty plaque	0%	60%	40%

Predictability of the mechanical property of plaque by IVUS. Table I shows the stiffness constant (K) for each group as classified by IVUS descriptors. The stiffness constant did not significantly differ among the minimally diseased arterial wall, isolated hypoechogenic plaque, and isolated bright echogenic plaque without shadowing (5.2 ± 0.7, 6.7 ± 1.6, and 6.2 ± 1.9, respectively). The stiffness constant for isolated bright echogenic plaque with shadowing (13.1 ± 5.1) was significantly greater ($p < 0.0005$) than the other echogenic patterns. The stiffness constant for hypoechogenic plaque and for bright echogenic plaque without shadowing was significantly greater ($p < 0.05$) than that of pure adipose tissue (2.8 ± 1.1).

The objective echo intensity index significantly correlated with the stiffness constant for all the combined groups (bright echogenic with or without shadowing and hypoechogenic plaques, $r = 0.71$, $p < 0.0005$), but a large overlap between hypoechogenic plaque and bright echogenic plaque without shadowing existed (Fig. 5).

Histologic validation. Table II illustrates the accuracy of the IVUS descriptors in identifying the composition of atherosclerotic plaque compared with histologic examination. Calcified plaque was detected with high sensitivity (91%), but discrimination between fibrous and fatty plaque on the basis of intensity of the echo signal was not very accurate (sensitivity 50% and 40%, respectively).

Table III shows the mean stiffness constants for the plaques when they were segregated by their histologic classification. Although the stiffness constant was significantly higher for calcified plaque, fibrous plaque and fatty plaque did not significantly differ. All the samples of apparently normal arteries by IVUS had histologic evidence of minimal intimal hyperplasia, but the intimal thickness of each specimen was <150 μm.

DISCUSSION

The major findings of this study are (1) the stress-strain relation of peripheral arterial plaque is non-

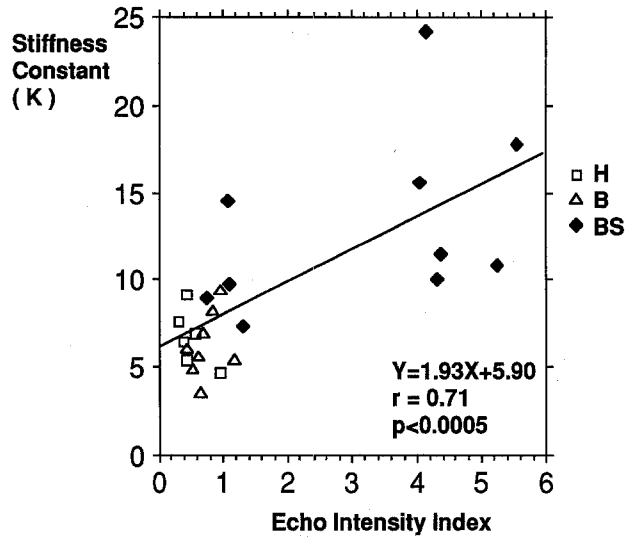

Fig. 5. Relation between objective echo intensity index and stiffness constant *(K)* of plaque. *BS*, Bright echogenic plaque with shadowing; *B*, bright echogenic plaque without shadowing; *H*, hypoechogenic plaque.

linearly exponential; (2) IVUS is able to distinguish the mechanical tissue characteristics of calcification from noncalcified tissue on the basis of the echogenicity of plaque; and (3) although noncalcified plaque has a lower stiffness constant than calcified plaque, noncalcified tissues are not physically soft compared with adipose tissue. The echogenic pattern of bright echoes without shadowing has the same stiffness constant as hypoechogenic plaque. Therefore soft echoes, although less firm than calcium, do not necessarily correspond to soft tissue.

The compressibility of tissue is correlated with ultrasound velocity.[34, 35] Therefore hypothesizing that echogenicity may be related to the compressibility of tissue is reasonable. For example, calcification produces high echogenicity, and lipid produces low echogenicity.[36] Lee et al.[22] examined the relation between the static stiffness and echogenicity of aortic plaque with a linear model of stress-strain with Young's modulus. They found that the IVUS appearance of calcified plaque was related to its biomechanical properties, but their data showed no definitive discrimination in mechanical behavior between fibrous and nonfibrous tissues as defined by IVUS. They used a linear stress-strain model with a constant stress applied to abdominal aortic plaque; despite these differences in technique, their data is consistent with ours.

Several reasons for discordance between echogenicity and tissue composition may exist. Atherosclerotic plaque is frequently composed of various kinds of tissue that may be intermingled in a complex way,

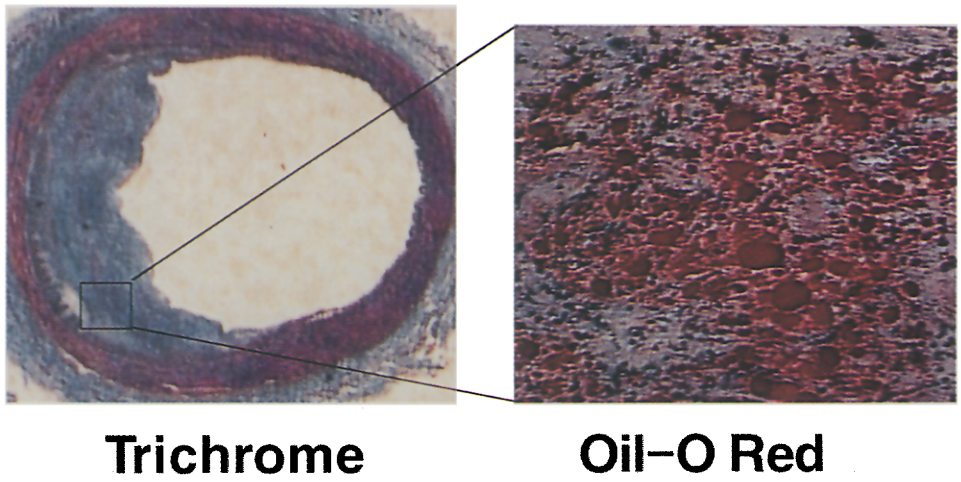

Fig. 6. Masson's trichrome stain and Oil-O red stain of mixed fibro-fatty plaque. Lipid content (red) is not homogeneous but is interspersed within matrix of fibrous tissue.

Table III. Stiffness constant (K) for each group classified by histologic examination

		Histologic class			
	Adipose tissue	*Minimally diseased entire arterial wall*	*Fibrous plaque*	*Fatty plaque*	*Calcified plaque*
K	2.8 ± 1.1	5.2 ± 0.7	5.9 ± 1.4	6.7 ± 2.0	12.6 ± 5.0*

Values are mean ± SD.
*Calcified plaque vs adipose tissue, minimally diseased entire arterial wall, or fibrous plaque, $p < 0.0001$; calcified plaque vs fatty plaque, $p < 0.0005$.

which could produce acoustic impedance mismatches inside the plaque.[36] Therefore the presence of lipid or collagen fiber does not always correspond to the overall echo intensity of the plaque.[37] The lower sensitivity of IVUS compared with histologic examination in discriminating fibrous and fatty tissue has been corroborated by previous histologic validation studies.[11, 14, 38, 39]

Another cause for disparity between plaque composition and IVUS characterization is interobserver variability of image interpretation. In a previous study, an assessment of tissue characterization showed only a moderate amount of agreement between two observers ($\kappa = 0.68$).[39] As shown in Fig. 5, some plaques identified by one observer as showing bright echogenicity (defined as an intensity of the plaque ≥ adventitia) did not have an echo intensity index ≥1.0 when the echo intensity was objectively measured by the brightness of the pixel gray scale. In addition, presentation of the same arterial cross section varies significantly among the available IVUS systems ($\kappa = 0.52$ between systems).[39]

In this study, even when the tissues were classified by histologic examination, fatty plaques were as firm as fibrous plaque, and both were firmer than pure adipose tissue. Several reasons for this overlap in the stiffness among groups may exist. First, the content of firm material such as collagen varies among plaques. Second, even fatty plaques consist of a matrix of collagen fibers, cells, and lipid, as demonstrated in Fig. 6. The greater specimen-to-specimen variability in stiffness of calcified plaques compared with noncalcified plaque is probably from variability in the degree of calcification within the plaque.[20] The minimally diseased entire arterial wall had a similar mean stiffness constant compared with isolated fibrous plaque from the adventitia that was left in place for the normal wall controls.

In conclusion, IVUS predicts the mechanical resistance to compression of atherosclerotic plaque and distinguishes whether the plaque contains calcium. However, this capacity is limited in discriminating between fibrous and fatty plaques. This limitation is caused by (1) the complex mixture of fibrous and fatty components within the plaque, (2) interobserver variability in interpretation of IVUS images, and (3) variability in image representation among IVUS systems from different companies.[39] Therefore physical descriptors such as "soft echoes" or "soft plaque" may be misleading when interpreting IVUS images. A nomenclature such as "calcified or noncal-

cified plaque" may be more appropriate to the experimental data. Alternatively, a description of the ultrasound image without extrapolation to histologic findings such as "bright echogenicity, with or without shadowing," and "hypoechogenic areas" would not presume that the echo image exactly corresponds to histologic findings or to the physical hardness of the tissue. These observations may have significant implications when using IVUS to guide coronary interventions or to choose an appropriate interventional device.

REFERENCES

1. Yock PG, Johnson EL, Linker DT. Intravascular ultrasound: development and clinical potential. Am J Card Imag 1988;2:185-93.
2. Gussenhoven EJ, Essed CE, Lancee CT, Mastik F, Frietman P, van Egmond FC, et al. Arterial wall characteristics determined by intravascular ultrasound imaging: an in vitro study. J Am Coll Cardiol 1989;14:947-52.
3. Tobis JM, Mallery J, Mahon D, Lehmann K, Zalesky P, Griffith J, et al. Intravascular ultrasound imaging of human coronary arteries in vivo. Analysis of tissue characterizations with comparison to in vitro histological specimens. Circulation 1991;83:913-26.
4. Mallery JA, Tobis JM, Griffith J, Gessert J, McRae M, Moussabeck O, et al. Assessment of normal and atherosclerotic arterial wall thickness with an intravascular ultrasound imaging catheter. Am Heart J 1990;119:1392-400.
5. Nissen SE, Grines CL, Gurley JC, Sublett K, Haynie D, Diaz C, et al. Application of a new phased-array ultrasound imaging catheter in the assessment of vascular dimensions: in vivo comparison to cineangiography. Circulation 1990;81:660-6.
6. Hodgson JM, Graham SP, Savakus AD, Dame SG, Stephens DN, Dhillon PS, et al. Clinical percutaneous imaging of coronary anatomy using an over-the-wire ultrasound catheter system. Int J Card Imaging 1989;4:187-93.
7. Pandian NG, Kreis A, Brockway B, Isner JM, Sacharoff A, Boleza E, et al. Ultrasound angioscopy: real-time, two-dimensional, intraluminal ultrasound imaging of blood vessels. Am J Cardiol 1988;62:493-4.
8. Potkin BN, Bartorelli AL, Gessert JM, Neville RF, Almagor Y, Roberts WC, et al. Coronary artery imaging with intravascular high-frequency ultrasound. Circulation 1990;81:1575-85.
9. Nissen SE, Gurley JC, Grines CL, Booth DC, McClure R, Berk M, et al. Intravascular ultrasound assessment of lumen size and wall morphology in normal subjects and patients with coronary artery disease. Circulation 1991;84:1087-99.
10. Nishimura RA, Edwards WD, Warnes CA, Reeder GS, Holmes DR, Tajik AJ, et al. Intravascular ultrasound imaging: in vitro validation and pathologic correlation. J Am Coll Cardiol 1990;16:145-54.
11. Di Mario C, The SH, Madretsma S, van Suylen RJ, Wilson RA, Bom N, et al. Detection and characterization of vascular lesions by intravascular ultrasound: an in vitro study correlated with histology. J Am Soc Echocardiogr 1992;5:135-46.
12. Friedrich GJ, Moes NY, Muhlberger VA, Gabl C, Mikuz G, Hausmann D, et al. Detection of intralesional calcium by intracoronary ultrasound depends on the histologic pattern. Am Heart J 1994;128:435-41.
13. Bartorelli AL, Potkin BN, Almagor Y, Keren G, Roberts WC, Leon MB. Plaque characterization of atherosclerotic coronary arteries by intravascular ultrasound. Echocardiography 1990;7:389-95.
14. Peters RJ, Kok WE, Havenith MG, Rijsterborgh H, van der Wal AC, Visser CA. Histopathologic validation of intracoronary ultrasound imaging. J Am Soc Echocardiogr 1994;7:230-41.
15. Mintz GS, Pichard AD, Kovach JA, Kent KM, Satler LF, Javier SP, et al. Impact of preintervention intravascular ultrasound imaging on transcatheter treatment strategies in coronary artery disease. Am J Cardiol 1994;73:423-30.
16. Keren G, Pichard AD, Kent KM, Satler LF, Leon MB. Failure or success of complex catheter-based interventional procedures assessed by intravascular ultrasound. Am Heart J 1992;123:200-8.
17. Matar FA, Mintz GS, Douek P, Farb A, Virmani R, Javier SP, et al. Coronary artery lumen volume measurement using three-dimensional intravascular ultrasound: validation of a new technique. Cathet Cardiovasc Diagn 1994;33:214-20.
18. Yock PG, Fitzgerald PJ, Sudhir K, Linker DT, White W, Ports A. Intravascular ultrasound imaging for guidance of atherectomy and other plaque removal techniques. Int J Card Imag 1991;6:179-89.
19. Colombo A, Hall P, Nakamura S, Almagor Y, Maiello L, Martini G, et al. Intracoronary stenting without anticoagulation accomplished with intravascular ultrasound guidance. Circulation 1995;91:1676-88.
20. Lee RT, Grodzinsky AJ, Frank EH, Kamm RD, Schoen FJ. Structure-dependent dynamic mechanical behavior of fibrous caps from human atherosclerotic plaques. Circulation 1991;83:1764-70.
21. Loree HM, Grodzinsky AJ, Park SY, Gibson LJ, Lee RT. Static circumferential tangential modulus of human atherosclerotic tissue. J Biomech 1994;27:195-204.
22. Lee RT, Richardson SG, Loree HM, Grodzinsky AJ, Gharib SA, Schoen FJ, et al. Prediction of mechanical properties of human atherosclerotic tissue by high-frequency intravascular ultrasound imaging. An in vitro study. Arterioscler Thromb 1992;12:1-5.
23. Gerritsen GP, Gussenhoven EJ, The SH, Pieterman H, v d Lugt A, Li W, et al. Intravascular ultrasonography before and after intervention: in vivo comparison with angiography. J Vasc Surg 1993;18:31-40.
24. The SH, Gussenhoven EJ, Zhong Y, Li W, van Egmond F, Pieterman H, et al. Effect of balloon angioplasty on femoral artery evaluated with intravascular ultrasound imaging. Circulation 1992;86:483-93.
25. Davidson CJ, Sheikh KH, Kisslo KB, Phillips HR, Peter RH, Behar VS, et al. Intracoronary ultrasound evaluation of interventional technologies. Am J Cardiol 1991;68:1305-9.
26. Hodgson JM. Morphology. In: Atlas of intravascular ultrasound. New York: Raven Press, 1994:32-7.
27. Gussenhoven WJ, Essed CE, Frietman P, Mastik F, Lancee C, Slager C, et al. Intravascular echographic assessment of vessel wall characteristics: a correlation with histology. Int J Card Imaging 1989;4:105-16.
28. Hodgson JM, Reddy KG, Suneja R, Nair RN, Lesnefsky EJ, Sheehan HM. Intracoronary ultrasound imaging: correlation of plaque morphology with angiography, clinical syndrome and procedural results in patients undergoing coronary angioplasty. J Am Coll Cardiol 1993;21:35-44.
29. Keren G, Douek P, Oblon C, Bonner RF, Pichard AD, Leon MB. Atherosclerotic saphenous vein grafts treated with different interventional procedures assessed by intravascular ultrasound. Am Heart J 1992; 124:198-206.
30. Rasheed Q, Dhawale PJ, Anderson J, Hodgson JM. Intracoronary ultrasound-defined plaque composition: computer-aided plaque characterization and correlation with histologic samples obtained during directional coronary atherectomy. Am Heart J 1995;129:631-7.
31. Rasheed Q, Hodgson JM. Application of intracoronary ultrasonography in the study of coronary artery pathophysiology. J Clin Ultrasound 1993;21:569-78.
32. Rasheed Q, Nair R, Sheehan H, Hodgson JM. Correlation of intracoronary ultrasound plaque characteristics in atherosclerotic coronary artery disease patients with clinical variables. Am J Cardiol 1994; 73:753-8.
33. Gussenhoven EJ, Essed CE, Frietman P, van Egmond F, Lancee CT, van Kappellen WH, et al. Intravascular ultrasonic imaging: histologic and echographic correlation. Eur J Vasc Surg 1989;3:571-6.
34. Curry TS III, Dowdey JE, Murry RC Jr. Ultrasound. In: Physics of diagnostic radiology. Philadelphia: Lea & Febiger, 1990;323-71.
35. Bushberg JT, Seibert JA, Leidholdt EM Jr, Boone JM. Ultrasound. In: The essential physics of medical imaging. Baltimore: Williams & Wilkins, 1994;367-416.
36. Barzilai B, Saffitz JE, Miller JG, Sobel BE. Quantitative ultrasonic characterization of the nature of atherosclerotic plaques in human aorta. Circ Res 1987;60:459-63.
37. Behan M, Kazam E. The echographic characteristics of fatty tissue and tumors. Radiology 1978;129:143-51.
38. Kerber S, Fechtrup C, Budde T, Fahrenkamp A, Bocker W, Breithardt G. Validation of intravascular ultrasound in arteriosclerotic peripheral vessels. Int J Cardiol 1994;43:191-8.
39. Hiro T, Leung CY, Russo RJ, Gutfinger DE, Farvid AR, Karimi H, et al. A comparison of four intravascular ultrasound imaging systems [abstract]. Circulation 1994;90:I-551.